This is a new one
IS-M-663
[redacted]

FIFTH INTERNATIONAL CONFERENCE ON HADRONIC MECHANICS AND NONPOTENTIAL INTERACTIONS

August 13-17, 1990 at University of Northern Iowa, Cedar Falls IA

ROUTE TO

NAME	LOCATION
RETURN TO PERS	

NONPERTURBATIVE BEHAVIOR OF QUARKS

K. E. Lassila

Physics Department and Ames Laboratory-DOE, Iowa State University, Ames, Iowa 50011

ABSTRACT

Several experiments have established that quarks exhibit different aspects of their interactions depending on their environment when they are probed. The nonlinear behavior found in nuclei is treated by expanding the many quark nuclear state as a series in color singlet multiquark states. The effects found in numerous nuclear target experiments can all be described by including the first two terms in this multiquark expansion. Comparisons with data from deep inelastic scattering by electrons, muons, neutrinos and antineutrinos will be given and also comparisons with dimuon production by protons on nuclei will be examined. Dilepton depletion at small target parton momentum fraction in proton-nucleus collisions will also be discussed as an example ot this nonlinear behavior.

I. INTRODUCTION

Quantum Chromodynamics (QCD) describes the behavior of interacting quarks and gluons which carry the quantum number named *color* in analogy with the three primary colors of visible light. Calculations have been done with high predictive power for situations with energetic or hard quarks or gluons. Indications are that these partons of QCD theory behave differently in different circumstances or environment. The surroundings in which a quark finds itself in a nucleus produce distortions of the quark distribution functions which have not been taken into account in past efforts to deduce nucleon structure functions from nuclear target data. The usual approach has been to assume that the nucleus of atomic number A is made of A free nucleons; this assumption has been proven wrong and the nuclear environment must be accounted for before structure functions can be deduced.

The data of the European Muon Collaboration (EMC) first showed that quarks in nuclei behave differently than those in free nucleons;[1] and, this result (the EMC effect) has been corroborated by a number of experiments with both electron and muon beams.[2] A prominant feature of these data is a pronounced reduction in the value of $F_2^{-1}(x)$, the deep inelastic structure function per nucleon measured on a nucleus (A), at

small momentum fraction $x < 0.1$, relative to the corresponding quantity measured on deuterium (D) $F_2^{D}(x)$. Except for $x > 0.7$ $F_2^{D}(x)$ very nearly behaves like and is often assumed to be equivalent to F_2 for two free nucleons. The ratio of these two quantities, $F_2^{A}(x)/F_2^{D}(x)$, will be abbreviated $R_\gamma(A/D)$, with the subscript designating the virtual photon that couples to the charge of the quark (q). Data on different A targets show that $R_\gamma(A/D) < 1$ for $x < 0.1$, reaches a maximum with $R_\gamma(A/D) \geq 1$ near $x = 0.15$, attains another pronounced reduction below unity near $x = 0.6$ and finally rises so that $R_\gamma >> 1$ as $x \to 1$. It was shown[3] that parton effects resulting from clustering of nucleons to form color singlet Nq structures $(N = 6, 9, ...3A)$ gave contributions at all values of x very much like the observed deviations of $R_\gamma(A/D)$ from unity. This approach can be justified[4] mathematically by expanding the A-nucleon, many quark state function for the $3A$ quark system in terms of color singlet multiquark states

$$| \Psi_A(3Aq) >= a_1 \, | 3q > + a_2 \, | 6q > + a_3 \, | 9q > + ..., \tag{1}$$

with the expection that all physical effects can be accounted for in a complete expansion by appropriate choice of coefficients. We argue the the coefficients of such an expansion can be interpreted physically. In Ref. [3], we used data from $N = 2$ (meson) and $N = 3$ (nucleon) quark systems to give a plausible motivation for the properties of the $6q$ system. This led to predictions for the value and slope of R_γ at $x = 0$; and, since the parton distributions are consequently determined, we can make predictions for various processes from them. We shall examine lepton pair production from nuclear targets and argue that if the small x behavior of R_γ is of partonic origin our choice of parton distribution functions necessarily implies a small-x depletion of lepton pairs produced on nuclear targets. Similar results for neutrino experiments with nuclear targets likewise follow.

Since the discovery of the EMC effect, several different explanations have been suggested as the source of these differences between bound and free nucleons; it is important to examine them all because nuclear target data give much of the input from which the nucleon structure functions have been determined. Although we shall study the contributions from multiquark[3] clusters to the differences between free and bound nucleons, we first discuss the other explanations to develop feeling for how they are related to our work: (i) The contributions from Fermi motion[5] have been well studied, but questions still are raised. The Fourier transform of the wave function for a nucleon in the nucleus determines the momentum distribution (Fermi motion) of the nucleon in a bound state, which in turn distorts the collision kinematics from that with the nucleon at rest. This produces a rapid rise in the ratio $R_\gamma(A/D)$ at large x because the distributions in the denominator of this ratio become small compared to those in the numerator as $x \to 1$. (ii) Multiquark cluster probabilities can be calculated from these same wave functions as the overlap of one nucleon with others,[6] leading to a literal interpretation of the color singlet $| Nq >$ states as real clusters. The behavior of a particular quark or gluon in such an enlarged quark system (cluster) will necessarily be different than it is in a single nucleon. (iii) Since pions are exchanged between nucleons in the nucleus, the deep inelastic process will occasionally probe pions and consequently produce a distortion which must likewise be taken into account.[7] The data require other effects also. (iv) The bound state character of the probed nucleon in the nucleus leads to a rescaling of the definition of the parton momentum fraction distribution. Numerous earlier studies of this specific contribution are summarized in [8] with the conclusion reached that "the nuclear binding and the nucleon Fermi motion in the convolution model of nucleons can not explain the EMC effect." (v) Overlapping of the parton wave functions in adjacent nucleons can occur when the partons have very small x values,[9] but this is what happens when a multiquark cluster is formed. Thus, there is considerable overlap between the different approaches. (vi) Hypothetical Q^2 rescaling effects for a bound nucleon may also contribute in certain kinematic regions.[10] (vii) Also, it has been argued that nucleon correlations contribute to the

EMC effect.[11] We believe that clusters may account for the major effects attributed to correlations as backward production of hadrons in neutrino reactions can be quantitatively described by the present approach.[12] Actually, most of the above effects are not mutually exclusive; as discussed above, in an extended version of the quark cluster model, an expansion of nuclear observables in terms of the set of states in Eq. (1) may be able to account for all the data.

Since the effects (i)-(vii) all have physical basis and some give contributions in specific kinematic regions, it seems important to understand all of them to appreciate their overlap with the cluster picture to see if our choice of parametrization can indeed incorporate the (possibly) different physics in this list.

The deviations[1] of $R_\gamma(A/D)$ from unity were shown[3] to result from differences in the regions of z in which valence $V(z)$ or ocean $O(z)$ quarks in N quark clusters make their contributions. We denote by z the scaled momentum fraction, e.g., $z = x$ for the 3q nucleon and $z = x/2$ for a 6q two nucleon color singlet cluster since a given quark can have a maximum value $z = 2$. For a generic N quark cluster we write[3]

$$O_N(z) = A_N(1-z)^{a_N}, \quad V_N(z) = B_N\sqrt{z}(1-z)^{b_N}, \quad G_N(z) = C_N(1-z)^{c_N}, \tag{2}$$

for the ocean, valence, and gluon distributions, respectively. The six parameters in Eq. (1) were determined from normalization to N valence quarks, momentum conservation constraints, and by examining data for $N = 2$ (pion) and $N = 3$ (nucleon) clusters, from which the ratio of momentum in the ocean to that in valence quarks could be fixed as independent of N. With the physically reasonable requirement that $a_N > b_N$, it is logical to take a_6 to be approximately in the range 11 - 13. This led to a satisfactory representation of the data[1,2] for the ratio $R_\gamma(A/D)$, as shown in Fig. 1, these curves

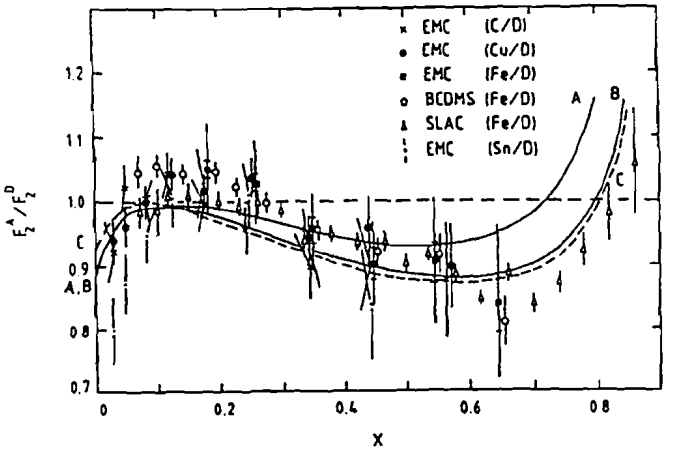

Fig. 1. Data[1,2] on the structure function ratio $R_\gamma(A/D)$ plotted vs quark momentum fraction x. The curves are labelled A, B, and C as defined in Eq. (3) in Ref.[3]. The resulting coefficients in Eq. (2) are $A_N = 0.222$, $B_N = 1.094$ for the nucleon and $(A_6, B_6) = (0.286, 1.762), (0.286, 1.850), (0.333, 1.850)$ for the $6q$ cluster in cases A, B, C, respectively.

being characterized by the three parameter sets

$$A = A(3,9,9,11),\ B = B(3,9,10,11),\ C = C(3,9,10,13), \tag{3}$$

where the quantities in parentheses signify $b_{v}, a_{3}, b_{G}, a_{G}$, respectively. In the calculations in Sect. II, we shall generalize b_{v}, the generic exponent of $(1-x)$ for the nucleon valence quarks, to be $b_{vu} = 3$ for the u quark and $b_{vd} = 4$ for the d quark. This has no effect on the analysis in [3], and minor effects in the following. Thus, the content of Eq. (3) can be rewritten

$$A = A([3,4],9,9,11),\ B = B([3,4],9,10,11),\ C = B([3,4],9,10,13), \tag{4}$$

where the numbers in parentheses signify $[b_{vu}, b_{vd}], a_{3}, b_{G}, a_{G}$. The gluon functions will not be required in the following. Each of these three sets of values (A, B, C) led to values of $R_{\gamma}(A/D)$ at $x \simeq 0$ which were less than unity. In numerical evaluations these three sets of parameters are specified as (A, B, C) and label appropriate curves as in Fig. 1. In the dilepton pair data comparisons, curves for case A will not be presented because its predictions are like those for case B.

II. DRELL-YAN DILEPTON PRODUCTION BY PROTONS ON NUCLEI

It has been pointed out that the Drell-Yan (DY) process can be a good source of information on quark and antiquark structure functions in nuclei.[13,14] For our purposes, it is clear that if nucleons in nuclei form quark clusters, there should be evidence of them in $q\bar{q}$ annihilation to lepton pairs in hadron-nucleus collisions. The authors of Ref. [13] have already noted this, and their calculations used the parton distributions of Carlson and Havens[4] which resulted in enhancement near $x = 0$. The following calculations update Ref. [13] with the parton distribution input from Eq. (4) above. This input, as seen in Figs. 2 and 3, produces a depletion at low x; this depletion (often referred to as "shadowing") results from the interplay between nucleon and cluster contributions in the nucleus.

We denote x_1 (x_P in Fermilab experiment E772 [15]) as the momentum fraction of the projectile (proton) that is carried by the annihilating quark [antiquark] and x_2 (x_t in [15]) as the momentum fraction carried by the antiquark [quark] that was annihilated in the target. The annihilation produces a photon of four-momentum squared, Q^2, equal to the mass squared, M^2, of the lepton pair into which the photon decays. The double differential (DY) cross section in these variables is a sum over all quark flavors a in the projectile[13]

$$\frac{d^2\sigma}{dx_1 dx_2} = \frac{4\pi\alpha^2}{9M^2}\sum_a e_a{}^2 F_a(x_1, x_2), \tag{5}$$

where e_a is the charge in units of proton charge, α is the fine structure constant, M^2 is the square of the mass of the lepton pair, and

$$F_a(x_1, x_2) = q_a{}^P(x_1)\bar{q}_a{}^t(x_2) + \bar{q}_a{}^P(x_1)q_a{}^t(x_2). \tag{6}$$

The quark [antiquark] distributions in the incident proton (P) or in the target (t) for parton a are $q_a{}^{P,or\,t}(x_{1,or\,2})$ [$\bar{q}_a{}^{P,or\,t}(x_{1,or\,2})$]. With the transverse momentum of the lepton pair also neglected[15] the product, $x_1 x_2 = M^2/s = \tau$, where s is the hadron-hadron center-of-momentum frame energy squared. We have $x_F = x_1 - x_2$ as the fraction of the maximum possible momentum for the dilepton pair. For fixed x_1, we form the ratio of the DY cross section per nucleon for target A divided by the corresponding quantity on target D and plot this ratio, $R_{DY}(A/D)$ as a function of x_2 to compare with experiment. In this ratio the Q^2 dependence from QCD predominantly cancels. In the target (A or D), the annihilating parton can be in a nucleon or a larger quark cluster. This probability for finding the neutron and proton overlapping to form a $6q$ cluster in the deuteron will be taken as 4%.[6]

The calculations we shall present are relevant for the discussion of the results of Fermilab experiment E772[15] which detected lepton pairs produced by proton beams incident on various nuclear targets: carbon(C), calcium(Ca), iron(Fe), and tungsten(W). The results have been presented as a ratio relative to the corresponding yield from deuterons. Some of our calculations showing a depletion in dilepton production at small x were presented previously and brief reports were published in various conference proceedings.[16,17,18] We have indicated that any parton structure function approach which gives small-x shadowing in deep inelastic scattering (DIS) necessarily gives shadowing in the DY process also. Our results appeared to be in conflict with preliminary[19] results from E772 but are in close agreement with the final experimental data. For the DY process, at very large x_1 we find that the value of $R_{DY}(A/D; x_2 = 0) = R_{\gamma}(A/D; x = 0)$ for the cluster contribution only; the other effects mentioned in Sect. I (e.g., pions) will modify this somewhat. In our present calculations, we do not assume x_1 is large but sum over all partons in the projectile that might contribute. Because this sum will not factor the same way in the numerator and denominator for DY, these two ratios will be approximately equal rather than exactly equal. But, at larger x_1 the stronger statement can be made: If there is depletion near $x_2 = 0$ in the DIS process, there will necessarily be depletion in DY production for shadowing of partonic origin.

In Figs. 2 and 3, we show the DY ratios for specific x_1 values calculated using

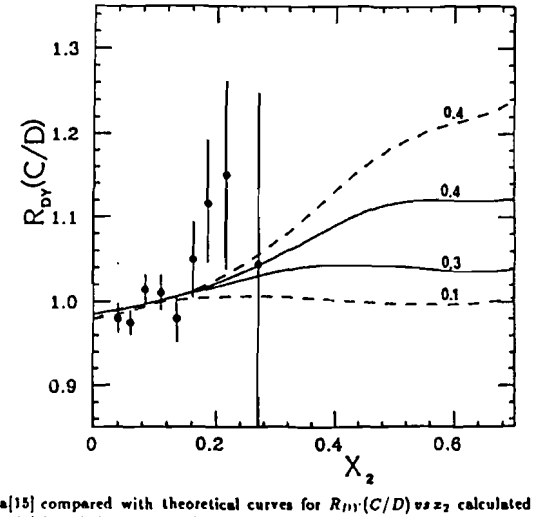

Fig. 2. Data[15] compared with theoretical curves for $R_{DY}(C/D)$ vs x_2 calculated for cases defined in Eqs. (2) and (4) with B given by the dashed lines and C given by the solid lines for the values of x_1 labelled on the curves. Curves for case A are the same as those for B for values of $x_2 < 0.4$ and differ very little from B for larger x_2. In the text, we refer to the dashed curves as $B(x_1 = 0.1)$ and $B(x_1 = 0.4)$, with the solid curves being $C(x_1 = 0.3)$ and $C(x_1 = 0.4)$.

Eqs. (2) - (6) for carbon and iron targets. The dot-dashed line on Fig. 3 was calculated and presented by the E772 experimenters as the prediction of the cluster model based on their assumptions for parton distributions within clusters.

The problem of interpretation of curves calculated for different x_1 values is the same for each target. We begin with the $R_{DY}(C/D)$ *vs* x_2 curves in Fig. 2 and apply the same analysis to the Fe data in Fig. 3. Carbon consists of 6 neutrons and 6 protons and we take the probability of cluster formation to be $f_C \simeq 0.1$.[6] The behavior of $R_{DY}(C/D)$, like any of the $R_{DY}(A/D)$, is such that for $x_2 > 0.1 - 0.2$, the value of R_{DY} increases as x_1 increases. From the information available in [15], it appears certain that the value of $x_1 = 0.4$ is large compared to most of the E772 data. Therefore, a number of curves for cases B and C for several different $x_1 \leq 0.4$ are shown compared with this data. Our presentation neglects the appropriate weighting of x_1 results for each x_2 bin because it is difficult to deduce the experimental weighting from [15]. Fortunately, the theory curves are very insensitive to the values of $x_1 \leq 0.4$ in the range where precision data exists. An excellent representation of the data will follow regardless of the weighting function in the experiment. The curves clearly predict depletion of dilepton pairs at small x_2, an effect confirmed at roughly the two and one half standard deviation level by the two smallest x_2 data points in Fig. 2. We show one curve explicitly for $x_1 = 0.3$ because this value can be interpreted as possibly being an effective average. This curve, $C(x_1 = 0.3)$ is more than adequate as a represention of the data. However, we emphasize again that whatever the correct weighting factor for doing an integration on x_1 from 0.05 to 0.4 or larger, the data will be well described by quark clusters in the nucleus. We leave open the possibility that the additional effects discussed in Sect. I might not be represented by the cluster expansion, Eq. (1), and whether agreement with the data might change.

At this point, it is useful to comment on the experimental dilepton mass distribution. The experimenters[15] show $d\sigma/dM$ falling by two orders of magnitude between

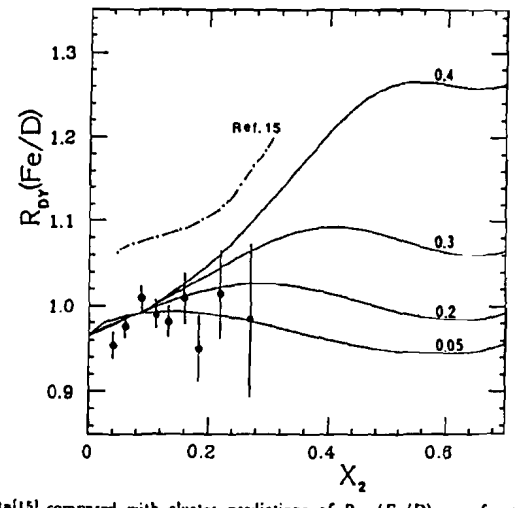

Fig. 3. Data[15] compared with cluster predictions of $R_{DY}(Fe/D)$ *vs* x_2 for case C with $x_1 = 0.05, 0.2, 0.3, 0.4$ (solid lines). The dot-dashed curve is the quark cluster curve from [15].

$M = 4$ and 9 GeV. If one normalizes to the cross section at any M value in this range, then the well-known $1/M^3$ scaling dependence multiplied by $ln ln(Q^2/Q_o^2)$ with $Q_o^2 = 4GeV^2$ gives a good representation of this non-resonant region data. Therefore, any theoretical description of this Drell-Yan process which is calculated from a QCD based interaction or parametrization of parton structure functions will be consistent with the $d\sigma/dM$ *vs* M dependence of the dilepton pairs. In particular, quarks and gluons in nucleons or $6q$ clusters in nuclei will likewise lead to this same relative mass variation.

For detailed comparison of our calculations of $R_{DY}(A/D)$ vs x_2 with the data, it is important to know the experimental x_1 variation. Lacking such information, we therefore have examined several approaches based on the experiment[15] which give us consistent answers. These considerations are summarized elsewhere[20], and here we simply say that curves for $x_1 = 0.3$ represent a reasonable average on which to base comparisons of theory with experiment.

Figure 3 shows the data[15] and theoretical curves for $R_{DY}(Fe/D)$ vs x_2 for several x_1 values. We note in comparing Figs. 2 and 3 that as A increases, f_A increases and the depletion of events relative to D becomes more marked. The precise values for f_A can not be predicted well; the values we used[6,20] are $f_{Fe} = 0.14, f_{Pb} = 0.18, f_W = 0.22$. There are indications that perhaps these probabilities should be larger for heavier nuclei as the calculations of Ref. [6] show that probabilities for the existence of $9q$, $12q$, etc., clusters grow with A; the effects of these larger clusters are included in an approximate way. Our comparisons with the calcium and tungsten target data are similar to those in Figs. 2 and 3 for carbon and iron and are therefore not included here.[20]

The comparison of the solid theory curves in Fig. 3 with data for $R_{DY}(Fe/D)$ vs x_2 proceeds exactly as discussed for Fig. 2. The dot-dashed curve is from the experimental paper[15] where it is represented as the prediction of a quark cluster model based upon parton distributions from [4]. The parton distributions of [4] were based on crude assumptions and those early applications did not provide a strong test of the ocean and gluon distributions. Clearly, our curves which are based on a quark cluster model, but with parton distributions determined by a systematic approach to the hadron target data, disagree markedly with the dot-dashed curve.

We note a very slow trend for the theory curves to show greater depletion or shadowing as x_1 increases. Conversely, for $x_2 > 0.1$, there is a slow increase of $R_{DY}(Fe/D)$ in the range of data as x_1 increases and this increase becomes dramatic beyond the range of data. These are predictions of the quark cluster model which can be tested by future experiment. Also, we note that if f_{Fe} is increased in the calculation to 0.3, the value of $R_{DY}(Fe/D; x_2 = 0)$ decreases by 0.4; in the framework of the cluster expansion this could amount to allowing enhanced shadowing of the type discussed by Qiu[9] to exist between soft partons in a cluster and partons in adjacent nucleons or clusters.

III. NONLINEAR BEHAVIOR PROBED WITH NEUTRINOS

Neutrino and antineutrino beam experiments have been used extensively to study quark momentum fraction distributions in nucleons. The incident ν turns into a μ^- plus a W^+ in the reaction with the W^+ raising the negatively charged d quark in a target nucleon into a u quark, with the possibility of the produced u quark jet and outgoing μ^- being detected. From a $\bar{\nu}$ beam, a μ^+ and W^- result and the W^- changes a u quark into a d quark; in this case, the produced μ^+ and/or the d quark jet would be detected. The almost unambiguous result of such data is direct information of the d (u) quark distribution in the target depending on whether ν ($\bar{\nu}$) beams were used. The small momentum fraction sea quarks would tend to obscure such a direct interpretation, but for larger x the valence quark function is clean. However, the overall result from data such as this, along with the deep inelastic scattering data discussed in Sect. I and the lepton pair data discussed in Sect. II is a set of equations which can be solved to

deduced the valence and sea quark distributions. The dilepton cross section is given in Eq. (5), depending linearly on both the structure in the projectile and the structure of the target. The data shown in Fig. 1 depends quadratically on the distribution in the target while the neutrino data varies linearly with the target distribution.

However, the experiments we have been describing have all been done on nuclear targets, especially those with neutrino beams, in order to enhance the cross sections. As we have seen, the presence of other quarks distorts the result relative to the free nucleon. Therefore, the assumption that the nucleus consists of A free nucleons when probed by high energy projectiles is simply wrong, and those analyses extracting quark and antiquark distributions based on this assumption are wrong.

If the neutrino beam experiments are done on nuclei and the behavior of quarks in nuclei is described by the cluster expansion of Eq. (1), what can be predicted for the neutrino beam experiments? The cross section for interactions of nuclei with ν or $\bar{\nu}$ beams can be expressed[21] in terms of structure functions in analogy with the discussion for the reactions in Sects. I and II. The F_2 structure function of deep inelastic electron or muon scattering is given by the quark distribution weighted by the quark charge squared. In the ν or $\bar{\nu}$ beam case, almost directly from the discussions

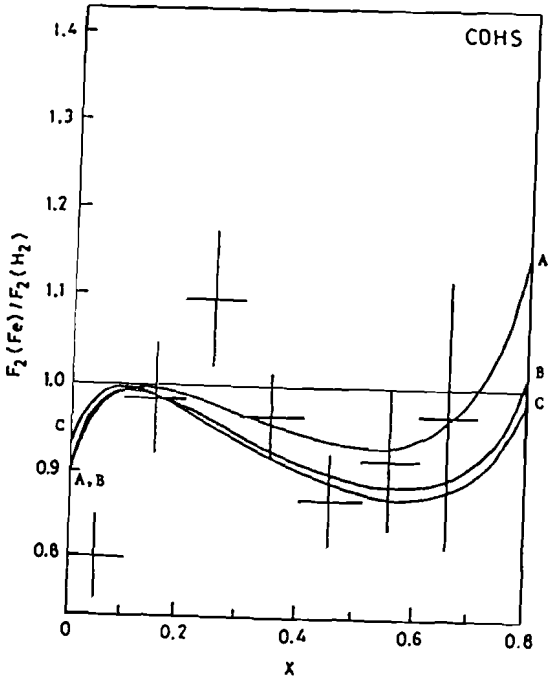

Fig. 4. Curves of $R_{\nu,\bar{\nu}}(A/D)$ vs x for cases (A, B, C) calculated from Eq. (9) compared with neutrino beam data[22].

in the previous paragraph, we[21] can write the analogous F_2 structure function in terms of up, down, strange, and charm (u, d, s, c) quark and antiquark distributions as

$$F_2^{\nu}(x) = 2[D(x) + S(x) + \bar{U}(x) + \bar{C}(x)], \tag{7}$$

$$F_2^{\bar{\nu}}(x) = 2[U(x) + C(x) + \bar{D}(x) + \bar{S}(x)]. \tag{8}$$

When we consider[21] that the partons may be in nucleons or $|6q>$ clusters, we can calculate the analogous ratio for these structure functions per nucleon in a nucleus A to that for the deuteron. This ratio is

$$R_{\nu,\bar{\nu}}(A/D) = 1 - f_A + f_A[6V(x/2) + 5\bar{U}_6(x/2)]/[6V(x) + 10\bar{U}_3(x)]. \tag{9}$$

In this expression, we adopted the notation of Eq. (2) for the valence quark with the sea quark distribution given as $\bar{U}_N = O_N/5$. This ratio from Eq. (9) is shown plotted in Fig. 4 compared with the CDHS[22] data; the theoretical curves are independent of ν, $\bar{\nu}$ beam type. These results demonstrate the same behavior seen in the other figures, with the shape being especially similar to that in Fig. 1.

IV. CONCLUSION AND DISCUSSION

The curves in Figs. 1-4 all illustrate consequences of the existence of quark clusters in nuclei. In dilepton production from nuclei, as x_1 increases, the value of the ratio $R_{DY}(A/D)$ decreases slightly at x_2=0 and increases considerably at larger $x_2 > 0.2$. The data[15] are not sufficiently precise to study such an effect in any detail. Performing an experiment with enough statistics to allow bins in x_1 to be plotted would *increase* our knowledge about the behavior of quarks in nuclei. With quark clusters forming in nuclei, it is clear that the major part of the increase in shadowing near $x = 0$ is explained by the increase in the number of possible quark clusters as the nucleon number increases. The values used,[6,20] $f_C = 0.1, f_{Ca} = 0.14, f_{Fe} = 0.18, f_W = 0.22$, were based on estimates of the overlap between nucleons from extrapolations in A, and have perhaps a 25 per cent error in them. This produces a 0.03 change in the value of R_{DY} at $x_2 = 0$ for the heavy nuclei. This uncertainty in f_A might be large enough that for a heavy nucleus like tungsten, $f_W = 0.3$ is possible. This uncertainty reflects our approximate treatment of clusters of 9, 12, etc., quarks in such a nucleus. Another source of deviation in the theory value comes from the intrinsic uncertainties in deducing the structure functions and the resulting feedback in getting the cluster distributions accurately. The uncertainty in f_A along with other uncertainties suggests the total theory error band on our calculated curves might be such as to be 0.04 - 0.05 wide in the plotted ratios throughout most of the x_2 or x range of the data on all the figures. We note that this 0.04 uncertainty in R_{DY} is small compared with the differences between our theory curves and the dot-dashed curve given in Fig. 3. We believe our curves are much more representative of the quark cluster model predictions than that presented[15] by the experimenters.

In conclusion, these comparisons with deep inelastic scattering, Drell-Yan and neutrino beam data supports the use of the cluster model as a plausible phenomenological description of the behavior of quarks in nuclei. Perhaps our analysis is now at the stage where we could make a much stronger statement as to quarks and gluons congregating into physical color singlet multiquark systems as real entities in nuclei (or in a plasma). At any rate, in the past, experimenters have usually treated the nucleus as a collection of free nucleons when extracting structure functions from nuclear target data. The cluster model approach provides a tool with which to remove nuclear effects and get more reliable parton distributions.

ACKNOWLEDGMENTS

I would like to thank Professor H. C. Myung and the other University of Northern Iowa staff for making this conference a success. Also, I am grateful for hospitality of and discussions with many colleagues, especially Drs. U. Sukhatme, C. E. Carlson, J. Qiu, and D. Sivers, at the HEP Division of Argonne National Laboratory where much of this work was done. We would like to acknowledge the support of the U. S. Department of Energy, Division of High Energy Physics, contract no. W-7405-ENG-82 Office of Energy Research (KA-01-01).

REFERENCES

[1] See, e.g., J. Ashman [EMC collaboration] et al., *Phys. Lett.* **202B**, (1988) 603 and J. J. Aubert et al., *ibid.* **123B**, (1983) 275.
[2] R. G. Arnold et al., *Phys. Rev. Lett.* **52**, (1984) 727; A. Bodek et al., *Phys. Rev. Lett.* **50**, (1983) 1431 and **51**, (1983) 534; G. Bari et al., *Phys. Lett.* **163B**, (1985) 282; A. C. Benvenuti et al., *ibid.* **189B**, (1987) 483; J. J. Aubert et al.,*Nucl. Phys.*B**259**, (1985) 189 and B**272**, (1984) 158.
[3] K. E. Lassila and U. P. Sukhatme, *Phys. Lett.* **209B**, (1988) 343
[4] C. E. Carlson, private communication; H. Pirner and J. P. Vary, *Phys. Rev. Lett.* **46**, (1981) 1376; C. E. Carlson and T. J. Havens, *Phys. Rev. Lett.* **51**, (1983) 261.
[5] A. Bodek and J. L. Ritchie, *Phys. Rev.D* **23**, (1981) 1070 and **24**, (1981) 1400. See also D. Kusno and M. J. Moravcsik, *Phys. Rev. D* **20**, (1978) 2734 and G. Yen, J. P. Vary, A. Harindranath, and H. J. Pirner, *Phys. Rev. C*,**42**, (1990) 1665 for earlier work and references.
[6] M. Sato, S. A. Coon, H. J. Pirner, and J. P. Vary, *Phys. Rev.C* **33**, (1986) 1062.
[7] E. L. Berger and F. Coester, *Ann. Rev. Nucl. Part. Sci.* **37**, (1987) 463; E. L. Berger, F. Coester, and R. B. Wiringa, *Phys. Rev. D* **29**, (1984) 398.
[8] G. L. Li, K. F. Liu ,and G. E. Brown, *Phys. Lett.* **213B**, (1988) 531.
[9] A. H. Mueller and J. Qiu, *Nucl. Phys.* **B268**, (1986) 427; J. Qiu, *ibid.* **B291**, (1987) 746; E. L. Berger and J. Qiu, *Topical Conf. on Nuclear Chromodynamics*, Ed. J. Qiu and D. Sivers (World Scientific, Teaneck NJ, 1988) p. 119; L. L. Frankfurt and M. I. Strikman, *Phys. Rep.* **160** (1988) 235; N. N. Nicolaev and V. I. Zakharov, *Phys. Lett.* **55B**, (1975) 397.
[10] F. Close et al., *Phys. Rev. D* **31**, (1985) 1004; F. E. Close, *Nucl. Phys.* **A478**, (1988) 407c.
[11] C. Ciofi della Atti and S. Liuti, *Phys. Lett.* **B225**, (1989) 215.
[12] C. E. Carlson, K. E. Lassila, and U. P. Sukhatme, *Backward Hadrons from Deep Inelastic Lepton Scattering* , preprint WM-90-115 (1990).
[13] A. Harindranath and J. P. Vary, *Phys. Rev. D* **34**, (1986) 3378.
[14] E. L. Berger, *Nucl. Phys.* **B267**, (1986) 231; R. P. Bickerstaff, M. C. Birse, and C. A. Miller, *Phys. Rev. Lett.* **53**, (1984) 2532 and *Phys. Rev.* **D33**, (1986) 3228.
[15] D. M. Alde et al., *Phys. Rev. Lett.* **64**, (1990) 2479.
[16] K. E. Lassila and U. P. Sukhatme, *Nuclear and Particle Physics on the Light Cone*, Ed. M Johnson and L. Kisslinger (World Scientific, NJ 1989) p. 115.
[17] K. E. Lassila, A. N. Petridis, C. E. Carlson, and U. P. Sukhatme, *Proceedings of the American Physical Society Division of Particles and Fields Meeting at Rice University*, Ed. W. Bonner and H. E. Miettinen, in press.
[18] K. E. Lassila and U. P. Sukhatme, *Small-x Shadowing in Dimuon Production*, submitted to *Phys. Lett.*, 1990, and *Small-x Shadowing in Dimuon Production by Protons on Nuclei*, submitted to the *25th International Conference on High Energy Physics, Singapore* (1990).
[19] J. C. Peng, talk presented at the LAMPF Workshop, *Nuclear and Particle Physics on the Light Cone*, Ed. M. Johnson and L. Kisslinger (World Scientific, NJ 1989) p. 65.

[20] K. E. Lassila, U. P. Sukhatme, A. Harindranath, and J. V. Vary, *Dilepton Production by Protons on Nuclei and the Partonic Origin of Depletion at Small Momentum Fraction*, preprint IS-J 4052 submitted to Physical Review
[21] K. E. Lassila and U. P. Sukhatme, *Analog of the EMC Effect in Neutrino-Nucleus Interactions, Int. Journal of Mod. Phys. A*, in press.
[22] H. Abramowicz et al.,*Z. Phys. C* **25**, (1984) 29.